Electronic Supplementary Material (ESI) for Journal of Materials Chemistry A.

Supporting information

Efficient $CsSnI_3$-based inorganic perovskite solar cells based on mesoscopic metal oxide framework via incorporating donor element

*Tao Zhang, Hao Li, Huaxia Ban, Qiang Sun, Yan Shen, Mingkui Wang**

Wuhan National Laboratory for Optoelectronics, Huazhong University of Science and Technology, Wuhan 430074, P. R. China.

* Corresponding author. E-mail: mingkui.wang@mail.hust.edu.cn

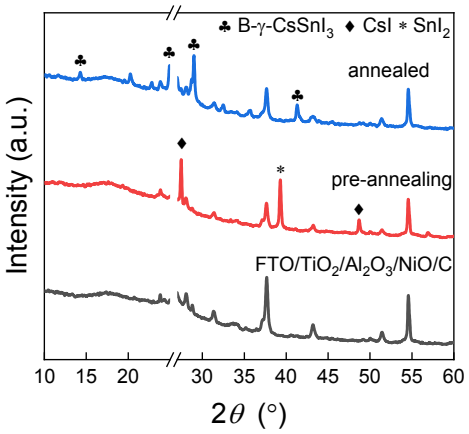

Figure S1. XRD plot of bare $CsSnI_3$ films before annealing and annealed at 70 °C on the FTO/TiO_2/Al_2O_3/NiO/C substrate.

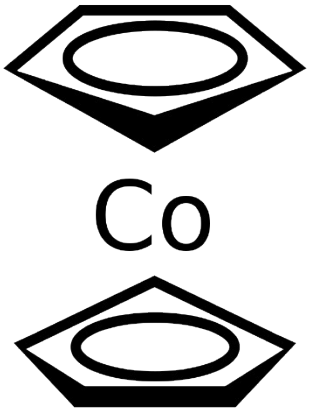

Figure S2. The molecular structure of cobaltocene (with the formula of $Co(C_5H_5)_2$). In $Co(C_5H_5)_2$ the Co center is "sandwiched" between two cyclopentadienyl (Cp) rings.

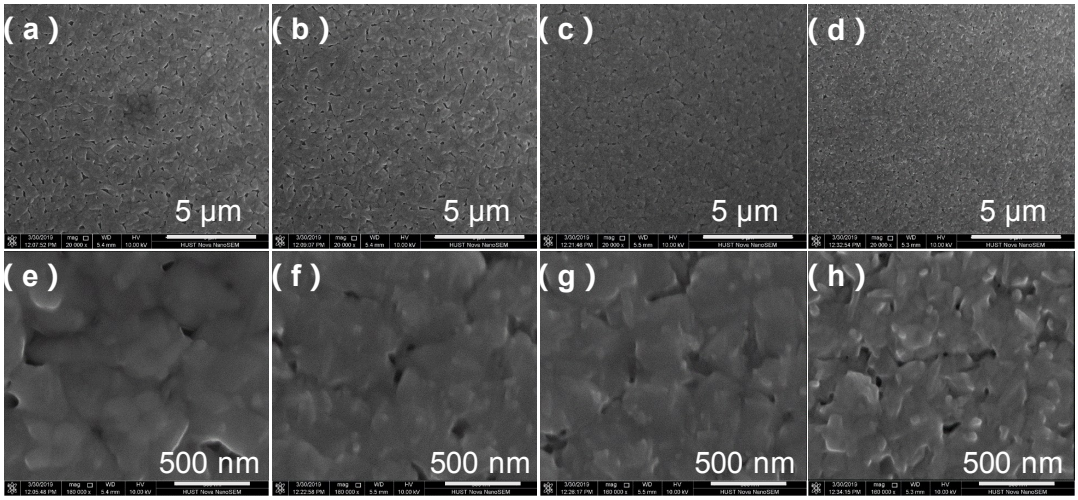

Figure S3. Top view SEM images of $CsSnI_3$ films without (a, e) and with (b, f) 0.5, (c, g) 1 and (d, h) 2% cobaltocene.

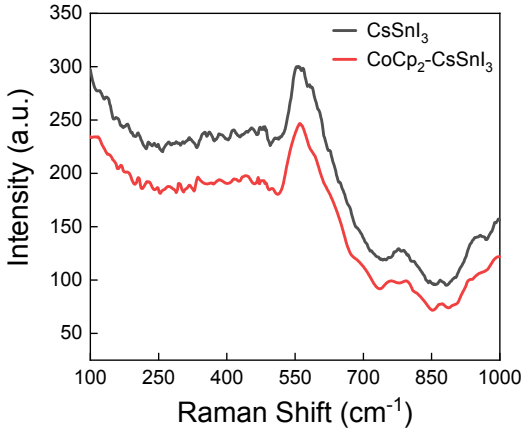

Figure S4. Raman spectra of pristine $CsSnI_3$ and $CoCp_2$-$CsSnI_3$ films.

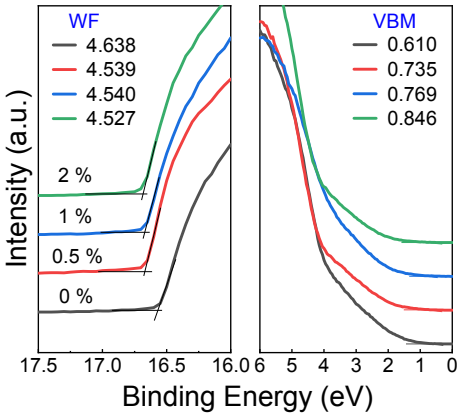

Figure S5. Ultraviolet photoelectron spectroscopy (UPS) characterization corresponding to the secondary electron onset region (WF, work function) and valence band region (VBM, valence band minimum) of the $CsSnI_3$ films with different $CoCp_2$ contents.

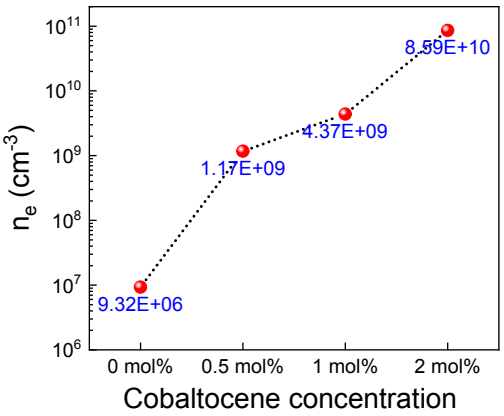

Figure S6. The calculated electron concentrations as a function of cobaltocene contents in $CsSnI_3$ films.

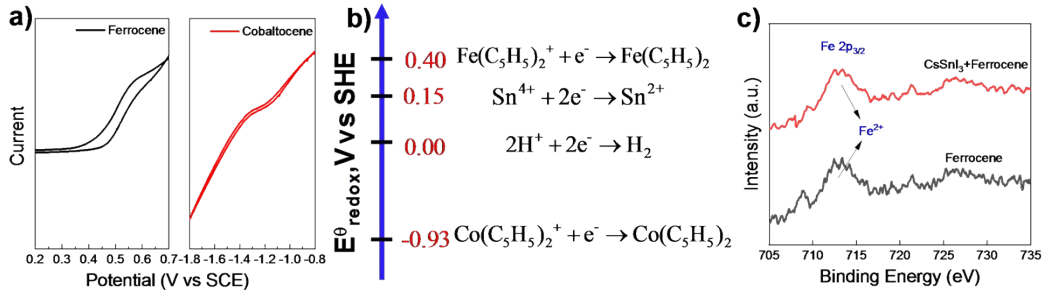

Figure S7. (a) Cyclic voltammetric scans for ferrocene and cobaltocene at a scan rate of 20 mV/s. The CV curves were obtained on a CHI-660C electrochemical workstation with Pt disk, Pt wire, and saturated calomel electrode (SCE) as working electrode, counter electrode, and reference electrode, respectively. (b) The reduction potentials of relevant materials, using the standard hydrogen electrode (SHE) as reference. The redox potential Sn^{4+}/Sn^{2+} were given in earlier report.[1] (c) High resolution XPS spectrum of the Fe 2p for $CsSnI_3$ films with and without ferrocene.

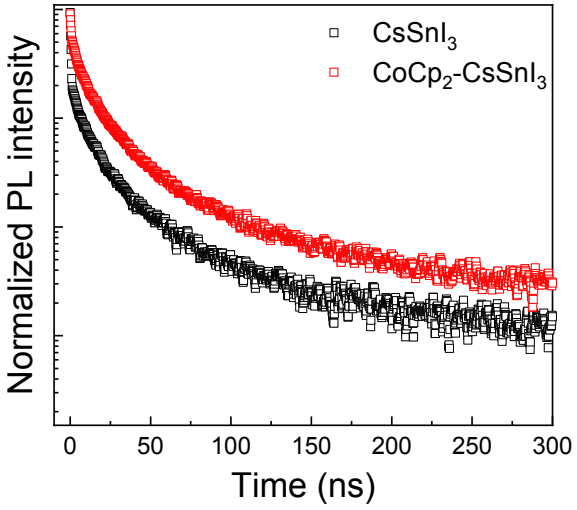

Figure S8. Time resolved PL spectra of the perovskite films incorporating bare $CsSnI_3$, $CsSnI_3$ with cobaltocene.

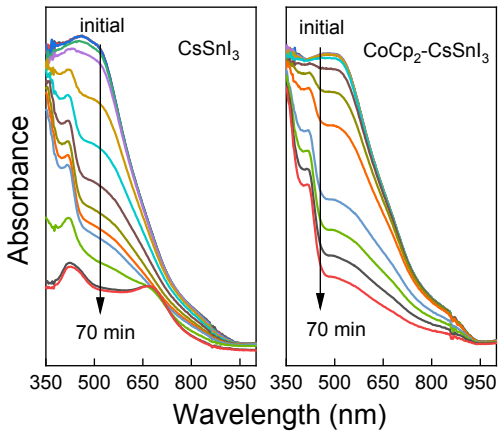

Figure S9. Absorbance of $CsSnI_3$ (left) and $CsSnI_3$ + 1% $CoCp_2$ (b) films. The black vertical lines indicate the direction of change with increasing time (every 5 minutes) in ambient air.

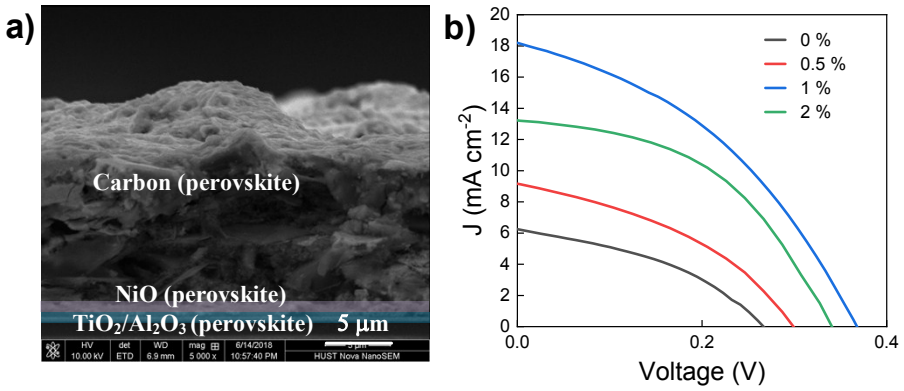

Figure S10. (a) Configuration of the PSCs from cross-sectional SEM image; (b) *J-V* curves of PSCs containing different amounts of cobaltocene.

Table S1. Comparison of the performance parameters of perovskite solar cells with different cobaltocene concentrations.

Devices	V_{OC}/V	Jsc/mA.cm^{-2}	FF/%	PCE/%
0 %	0.27	6.25	38.54	0.65
0.5%	0.31	9.14	37.45	1.07
1%	0.36	18.24	45.92	3.00
2%	0.34	13.23	46.93	2.11

Table S2. Comparison of the performance parameters of perovskite solar cells with different ferrocene concentrations.

Devices	V_{OC}/V	Jsc/mA.cm^{-2}	FF/%	PCE/%
0 %	0.27	6.25	38.54	0.65
0.5 %	0.31	7.92	33.57	0.81
1 %	0.32	4.57	36.24	0.54

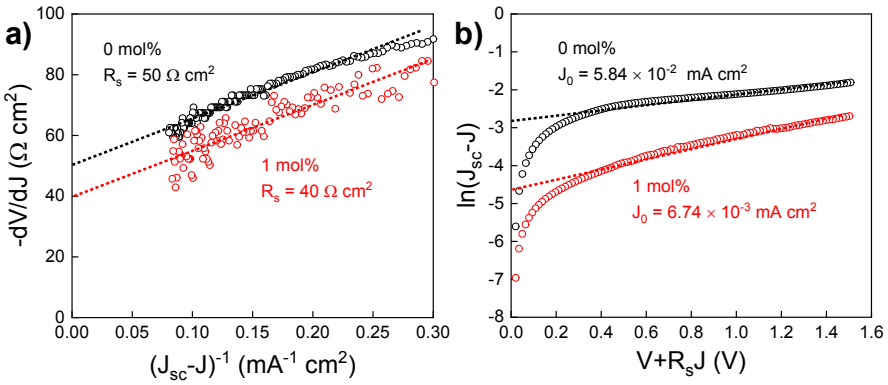

Figure S11. (a) Plots of -dV/dJ vs $(J_{SC}-J)^{-1}$ and the linear fitting curves, (b) plots of ln(J_{SC}-J) against V+R_SJ and the linear fitting curves.

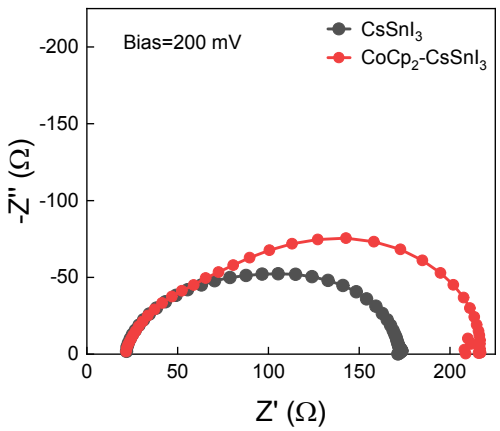

Figure S12. Nyquist plots of PSCs devices obtained under light at a bias voltage of 0.20 V.

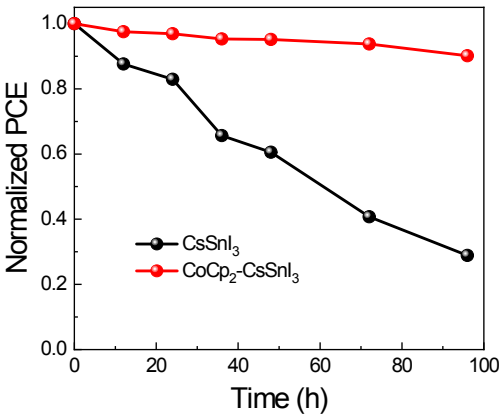

Figure S13. Normalized PCE of PSCs as a function of aging time in a nitrogen atmosphere.

Reference

1 Z. Zhu, N. Li, D. Zhao, L. Wang and A. K. Y. Jen, *Adv. Energy Mater.*, 2019, **9**, 2–9.